

STT-CBS: A Conflict-Based Search Algorithm for Multi-Agent Path Finding with Stochastic Travel Times

Oriana Peltzer¹, Kyle Brown¹, Mac Schwager², Mykel J. Kochenderfer², and Martin Sehr³

¹ Dept. of Mechanical Engineering, Stanford University, CA 94305, USA,
{peltzer,kjbrown7}@stanford.edu

² Dept. of Aeronautics and Astronautics, Stanford University, CA 94305, USA,
{schwager,mykel}@stanford.edu

³ Corporate Technology, Siemens Corporation, Berkeley CA 94704, USA,
martin.sehr@siemens.com.

Abstract. We address the Multi-Agent Path Finding problem on a graph for agents assigned to goals in a known environment and under uncertainty. Our algorithm, called STT-CBS, uses Conflict-Based Search (CBS) with a stochastic travel time (STT) model for the agents. We model robot travel time along each edge of the graph by independent gamma-distributed random variables and propose probabilistic conflict identification and constraint creation methods to robustly handle travel time uncertainty. We show that under reasonable assumptions our algorithm is complete and optimal in terms of expected sum of travel times, while ensuring an upper bound on each pairwise conflict probability. Simulations and hardware experiments show that STT-CBS is able to significantly decrease conflict probability over CBS, while remaining within the same complexity class.

Keywords: Multi-Agent Path Finding, Conflict-Based Search, Motion and Path Planning

1 Introduction

In many real-world applications, we are interested in routing a team of robots from an initial configuration to a target configuration through dynamically feasible and conflict-free paths. Relevant applications include real-time vehicle routing [19], warehouse management [16], and unmanned aerial vehicle (UAV) coordination [18]. A common formulation of this planning task is the Multi-Agent Path Finding (MAPF) problem, wherein agents are allowed to move along the edges of a graph from their initial locations to prescribed destinations. Recently, optimal MAPF planners have shown their effectiveness empirically on a large category of problems (e.g., [1, 13, 23]), most of which focus on deterministic travel times. In contrast, accounting for uncertainty in travel time due to environmental disturbances improves consistency and reliability in the actual execution of planned paths, preserving the low costs obtained through the optimization process.

We propose Stochastic Travel Time Conflict-Based Search (STT-CBS), a novel MAPF planning algorithm that seeks to minimize the sum of travel times of the robots subject to a bound on the probability of collision for any pair of robots. We model the travel time for each robot to traverse an edge of the graph⁴ as a gamma-distributed random variable. This model of randomness captures the sequential summing of uncertain effects along a trajectory of multiple edge traversals. We show that if a solution exists, our algorithm will return the solution that minimizes expected total travel time subject to the probabilistic collision constraint. We compare STT-CBS against a state-of-the-art baseline algorithm on a set of experiments, showing that our algorithm can better prevent collisions under this stochastic travel time model.

2 Background and Related Work

In the discrete-time MAPF formulation, edges can be traversed in unit time. This is sometimes called the “pebble motion” problem [6]. We consider the case in which each robot is assigned to a specific goal. This is often called the “labeled” case. The solution to a discrete-time MAPF problem is a joint assignment of trajectories such that no two agents are expected to occupy the same vertex or traverse the same edge at the same time. A solution is said to be *optimal* with respect to total travel time if it minimizes the sum of the lengths of all of the paths. We can use this objective when all tasks are equally important. Finding an optimal solution to the labeled discrete-time MAPF problem is NP-Hard [22]. Optimal and *complete* MAPF solution methods (those that are guaranteed to find an optimal solution if it exists) can be broadly grouped into three categories: In *coupled* approaches, the search for an optimal feasible solution is performed directly in the joint action space of the agents. *Decoupled approaches* operate by computing paths on an individual (per-agent) basis, and then resolving pairwise conflicts repeatedly by re-planning. This is the basis of Conflict-Based Search and its variants [1]. Some approaches are *semi-coupled*—they group agents into teams or “meta-agents”, and then apply a de-coupled approach between the joint plans associated with each team. A representative example of a semi-coupled approach is Operator Decomposition and Independence Detection (OD+ID) [14].

The “pebble-motion” MAPF formulation abstracts away robot dynamics and does not account for uncertainty. In trying to execute paths specified by a MAPF planner, actuator dynamics and other disturbances will inevitably introduce errors that violate the assumptions of constant-velocity and unit-time edge traversal. This can be problematic when nominally “conflict-free” trajectories are not conflict-free during actual execution. One way to address this modeling error is to ignore it during planning, and then to incorporate closed-loop control for stabilizing robots to the commanded trajectories [20]. While this approach can be highly effective, it relies on important spacing around agents in order to avoid

⁴ One can equivalently associate the delay with the edge e_{ij} or either of the two nodes for that edge, v_i or v_j . Without loss of generality, we choose to associate the delay with the end node v_j rather than the edge itself.

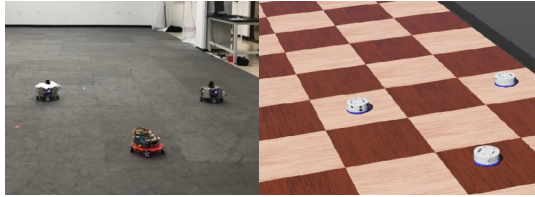


Fig. 1: Our algorithm plans collision-free paths in a graph for robots that travel with stochastic travel times along the edges. We evaluated the algorithm in hardware and simulation experiments with robots to verify the robustness of our approach to real-world stochastic delays.

cumulating delays and deadlocks. In warehouse design problems, there is a particular interest in minimizing clearance in between lanes in order to maximize space utilization [17]. To this end, we propose a solution that is able to perform more consistently in a cluttered environment.

The Conflict-Based Search (CBS) algorithm [1], a state-of-the-art algorithm to solve the optimal MAPF problem, has been widely studied and extended these last years. Many heuristics (e.g., [3,4]) have been developed to accelerate CBS. It has also been merged with different planning methods [12] and extended to more complex agent geometries [23] and graphs that allow for non-unit edge traversal times [5]. All suffer from the same problem as CBS, namely that the final solution is not necessarily robust to conflicts that might occur due to unmodeled delay in the actual execution of those paths.

Relatively few approaches actually reason about uncertainty during the planning phase. One example is k -robust CBS, which seeks solutions that remain collision free considering that each agent may be delayed for up to k time steps [10]. A downside of this model is that it fails to consider the sequential summing of delay as agents advance, which is especially important when the planning time horizon is large. UM* [24] introduces a more flexible model that takes this into account: agents' progress is modeled as a Markov Decision Process. This algorithm fits in the framework of M* [25], and provides an optimal planning solution for the MAPF problem within the pebble motion framework. However, the algorithm is not complete.

3 Approach

We consider the stochastic travel time MAPF problem under uncertain travel times. As in the deterministic travel time formulation, each agent must move from its initial location to a prescribed final location without collision with other agents. The task is to find a solution that minimizes the *expected* total travel time subject to the constraint that the likelihood of collision for each pair of agents at any place in the graph is below some threshold $\epsilon \in [0, 1]$.

3.1 Uncertainty Model

In warehouse / factory-floor settings, robots have low-level controllers that control them to track a desired path. However, disturbances are likely to occur as delays along the prescribed path due to wheel slip, feedback corrections from the low-level controller, unexpected minor obstacles, and other sources of stochastic delay. Our particular choice of travel time model is motivated by this phenomenon of stochastic accumulating delay for factory or warehouse robots.

We model delay as a random variable following a gamma distribution. More precisely, we consider that each time a node N_i is traversed by a robot, then the robot is delayed by a time ν_i , with $\nu_i \sim \text{Gamma}(n_i, \lambda)$. Then, the more nodes are traversed by each robot, the larger its expected delay becomes, and the less certain its position along its route in the graph. With the model described, we are able to encompass interactions in between robots at intersections, where they are the most likely to be delayed.

3.2 Conflict Probability

In this section, we express the probability of a conflict between two agents as a function of our model parameters. Figure 2 illustrates how a conflict can happen in this stochastic model, where planned arrival and departure times are not the same.

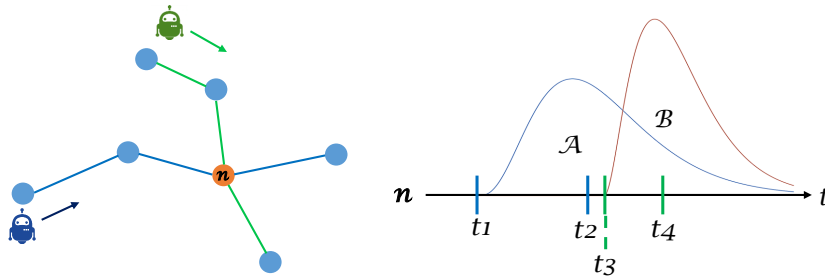


Fig. 2: Conflict identification at a node n . Blue and green robots are scheduled to traverse node n at different times. However, uncertainty over travel time may cause them both to reach node n at a time similar enough that they may collide. If the blue robot arrives at n before the green robot departs from n , and if the green robot arrives before the blue robot departs, then the robots will conflict with each other.

Cumulative delay Let $R1$ be an agent with an assigned route that we can write as a sequence of nodes and edges. At the start of its route, it is not delayed. As it traverses nodes, it accumulates delay ν_i , with $\nu_i \sim \text{Gamma}(n_i, \lambda)$.

For simplicity, we use a rate parameter λ that is identical across all the nodes in our graph. Conveniently, the sum of N independent gamma-distributed random variables with shape parameters n_i and identical rate parameter λ is a gamma-distributed random variable with shape parameter $\sum_{i=1}^N n_i$ and rate parameter λ . This helps us to write the delay accumulated by R1 as

$$\nu_{R1} \sim \text{Gamma}\left(\sum_{i=1}^N n_i, \lambda\right). \quad (1)$$

Using this stochastic delay, we can express the probability of a conflict between two robots, R1 and R2, at a particular node or edge.

Node Conflicts We consider a possible conflict at node m , which both R1 and R2 are scheduled to cross.

Let t_{A1} and t_{A2} be the nominal times at which robots R1 and R2 have planned to arrive at node m , respectively. The agents have accumulated delays ν_{R1} and ν_{R2} , according to equation (1). At node m , the agents will be delayed for times: $\nu_{D1}, \nu_{D2} \sim \text{Gamma}(n_m, \lambda)$.

R1 and R2 will conflict with each other if there exists a time interval during which they are both present at node m . We can write this in terms of the following events A and B :

- A : “agent R1 leaves after agent R2 arrives”
- B : “agent R2 leaves after agent R1 arrives.”

A conflict occurs if both inequalities A and B hold for a certain node and two agents R1 and R2. This is equivalent to

$$\begin{aligned} \text{Conflict} &\Leftrightarrow \begin{cases} t_{A1} + \nu_{R1} + \nu_{D1} \geq t_{A2} + \nu_{R2} & (A) \\ t_{A2} + \nu_{R2} + \nu_{D2} \geq t_{A1} + \nu_{R1} & (B) \end{cases} \\ &\Leftrightarrow \begin{cases} \nu_{R1} - \nu_{R2} \geq t_{A2} - t_{A1} - \nu_{D1} & (A) \\ \nu_{R1} - \nu_{R2} \leq t_{A2} - t_{A1} + \nu_{D2} & (B) \end{cases} \end{aligned}$$

Let $y = \nu_{R1} - \nu_{R2}$. Then, ν_{D1} and ν_{D2} (and therefore A and B) are conditionally independent given y , so we can write

$$P(\text{Conflict}) = P(A \cap B) = \int_y P(A | y)P(B | y)P(y)dy.$$

Writing $\text{Gamma}(x|n, \lambda)$ as $G(x|n, \lambda)$, we have

$$\begin{aligned} P(A | y) &= P(\nu_{D1} \geq t_{A2} - t_{A1} - y) \\ &= \int_{(t_{A2} - t_{A1} - y)^+}^{\infty} G(x|n_m, \lambda)dx. \end{aligned}$$

The same way,

$$\begin{aligned}
P(B | y) &= P(\nu_{D2} \geq t_{A1} - t_{A2} + y) \\
&= \int_{(t_{A1} - t_{A2} + y)^+}^{\infty} G(x|n_m, \lambda) dx.
\end{aligned}$$

We notice that for fixed t_{A1} , t_{A2} , and y , at least one of the two quantities $(t_{A2} - t_{A1} - y)^+$ or $(t_{A1} - t_{A2} + y)^+$ will be equal to 0. Therefore, at least one of $P(A | y)$ or $P(B | y)$ will be equal to 1. Consequently, we can simplify the product:

$$P(A | y)P(B | y) = \int_{|t_{A1} - t_{A2} + y|}^{\infty} G(x|n_m, \lambda) dx$$

Our next step is to express $P(y)$.

When $y \leq 0$,

$$P(y) = P_{neg}(y) = \int_0^{\infty} G(t|n_1, \lambda) \times G(t - y|n_2, \lambda) dt.$$

When $y > 0$,

$$P(y) = P_{pos}(y) = \int_0^{\infty} G(y + t|n_1, \lambda) \times G(t|n_2, \lambda) dt.$$

Finally, we can write that for a vertex,

$$\begin{aligned}
P(\text{Conflict}) &= \int_0^{\infty} P_{pos}(y) \int_{|t_{A2} - t_{A1} - y|}^{\infty} G(x|n_m, \lambda) dx dy \\
&\quad + \int_{-\infty}^0 P_{neg}(y') \int_{|t_{A2} - t_{A1} - y'|}^{\infty} G(x'|n_m, \lambda) dx' dy'.
\end{aligned} \tag{2}$$

We will denote this function $P(\text{Conflict}) = P_{cm}(t_{A1} - t_{A2}, n_1, n_2, \lambda, n_m)$.

Using this expression, we can numerically integrate the density over variable y . In order to speed up computation, we integrate in a smaller region surrounding the mode (which can be computed analytically) of this distribution.

Edge Conflicts We can similarly express edge conflicts for agents traversing the same edge in opposite directions. Let e be the edge in between nodes $N1$ and $N2$. Let us suppose that R1 traverses the edge from $N1$ to $N2$, and R2 traverses from $N2$ to $N1$. This edge takes time t_e to traverse.

We can designate t_{A1} as the time at which robot R1 has planned to leave node $N1$ and t_{A2} as the time robot R2 has planned to leave node $N2$.

With ν_{R1} the delay accumulated by R1 until node $N1$ and ν_{R2} the delay accumulated by R2 until $N2$, we can similarly express events A and B and write an edge conflict as follows.

$$\begin{aligned} \text{Conflict} &\Leftrightarrow \begin{cases} t_{A1} + \nu_{R1} + t_e \geq t_{A2} + \nu_{R2} & (A) \\ t_{A2} + \nu_{R2} + t_e \geq t_{A1} + \nu_{R1} & (B) \end{cases} \\ &\Leftrightarrow \begin{cases} \epsilon_{A1} \geq \nu_{R2} + t_{A2} - t_{A1} - t_e & (A) \\ \epsilon_{A1} \leq \nu_{R2} + t_{A2} - t_{A1} + t_e & (B) \end{cases} \end{aligned}$$

We can then write that on an edge,

$$\begin{aligned} P(\text{Conflict}) &= P_{ce}(t_{A1} - t_{A2}, n_1, n_2, t_2, \lambda, t_e) \\ &= \int_0^\infty G(e_2 | n_1, \lambda) \int_{(b-t_e)^+}^{(b+t_e)^+} G(x | n_2, \lambda) dx de_2 \end{aligned} \quad (3)$$

with $b = e_2 + t_{A2} - t_{A1}$.

Remark 1. Notice that under our model, computing the probability of conflicts on edges is relatively inexpensive compared to conflicts on nodes. Using the cumulative density function for the gamma distribution, the former only implies to integrate over one variable, here e_2 . The reason for this is that we do not introduce delay along edges.

Remark 2. In this paper, we assume that the random variables ν_{R1} , ν_{R2} , ν_{D1} , and ν_{D2} are mutually independent, which may not hold in applications where disturbances are likely to affect multiple robots at the same location. However, we can extend our approach to specific models in order to capture these effects. In fact, we can show that the conflict probability remains the same as long as the marginal distributions of ν_{D1} and ν_{D2} are preserved.

4 Algorithm

4.1 STT-CBS

STT-CBS uses the same high-level structure as CBS, reproduced in Algorithm 1. Our main contributions reside in conflict detection and resolution. The stochastic travel time model enables the algorithm to operate on simpler graphs where decomposition of time into time steps is not required. More specifically, nominal travel times at edges (or edge weights) can be arbitrary, in contrast with methods that constrain edge travel time to integers or unit time.

In the original CBS algorithm, conflicts are detected by searching all pairs of robots at each time step. In STT-CBS, we search each node and edge containing occupants that could conflict. For example, for each occupied edge, we consider all combinations of robots traversing in opposite directions. Algorithm 2 shows how the conflict detection process differs from CBS. We choose to expand our

Algorithm 1 High level of CBS and STT-CBS

```

Initialize root node  $\mathcal{R}$ :
 $\mathcal{R}.\text{constraints} \leftarrow \emptyset$ 
 $\mathcal{R}.\text{solution} \leftarrow$  Find low level solution to  $\mathcal{R}$  using A*
 $\mathcal{R}.\text{cost} \leftarrow$  Find solution cost
Insert  $\mathcal{R}$  into priority queue
while Priority Queue  $\neq \emptyset$ 
   $\mathcal{P} \leftarrow$  best node in Priority Queue
   $\mathcal{P}.\text{conflict} \leftarrow$  MostLikelyConflict( $\mathcal{P}$ )
  if  $\mathcal{P}$  is conflict-free
    Return  $\mathcal{P}.\text{solution}$ 
  for each agent  $a_i$  involved in  $\mathcal{P}.\text{conflict}.\text{agents}$ 
    Create child node  $\mathcal{C}$ 
     $\mathcal{C}.\text{constraints} \leftarrow \mathcal{P}.\text{constraints} +$  Constraint-From-Conflict( $\mathcal{P}.\text{conflicts}, a_i$ )
     $\mathcal{C}.\text{solution} \leftarrow$  Find low level solution to  $\mathcal{C}$  using A*
     $\mathcal{C}.\text{cost} \leftarrow$  Find solution cost
    Add  $\mathcal{C}$  to priority queue

```

constraint checking tree with the most likely conflict. We note that while evaluating the conflict probability at an edge, we search adjacent edges for occupancy information. This way, we ensure that we will not overlook likely edge conflicts due to overlapping paths.

Given a conflict between R1 and R2, one way to create the constraint “R1 yields to R2” is to calculate conflict probability with an increasing delay for R1. Then the time the agent should yield is the smallest delay that yields a probability smaller than ϵ . We use hyper-parameter Δt in order to gradually increase delay. Until the returned time, the yielding agent is not authorized to use the element (node or edge). Choosing a small value for Δt costs the algorithm additional iterations. However, if Δt is too large, we lose a key assumption that ensures the optimality of the returned solution. Empirically, we hand-tune this parameter according to our problem. We are also able to use binary search in order to find the yielding time that makes conflict probability as close as possible, and inferior to, ϵ more efficiently.

4.2 Properties

We will prove that under our model, as $\Delta t \rightarrow 0$, the solution returned is optimal in terms of expected sum of travel times. We will follow the same procedure as [1].

Definition 1 A solution p is valid if and only if each pairwise conflict probability, at each node and longest edge traversed by opposing robots, is smaller than a threshold ϵ .

Definition 2 For a given node N in the constraint tree, we will call $CV(N)$ the set of valid solutions that do not violate constraints of N .

Definition 3 A node N permits a solution p if and only if $p \in CV(N)$.

Algorithm 2 Most Likely Conflict

Fill the graph with occupancy information:
for each edge traversed by agents in S
 Add occupancy information to the graph at nodes and edges: agent R , expected arrival time t , shape factor n
 $P_{c_{max}} = \epsilon$
 MostLikelyConflict = \emptyset
for each occupied vertex and edge in the graph
for each of their pairwise, possibly conflicting occupants
if considered element is an edge
 Search for adjacent edges traversed by both agents
 Combine these edges
 Calculate $P_{conflict}$ using (2) or (3)
if $P_{conflict} \geq P_{c_{max}}$
 MostLikelyConflict = Conflict(concerned agents, planned times of arrival)
 $P_{c_{max}} = P_{conflict}$
return MostLikelyConflict

Lemma 1 *As $\Delta t \rightarrow 0$, each resolved constraint ensures that the corresponding collision probability tends towards ϵ .*

Proof.

Node constraints For fixed t_{A2}, n_1, n_2 , the function f mapping $t_{A1} \in \mathbb{R}^+$ to $f(t_{A1}) = P_{cm}(t_{A1} - t_{A2}, n_1, n_2, \lambda, n_m)$ is a continuous function of t_{A1} . We show that $f(t_{A1}) \rightarrow 0$ when $t_{A1} \rightarrow \infty$ (the same applies for t_{A2}).

Using the expression of node conflict probability in Section II, we will first show that

$$\lim_{t_{A1} \rightarrow \infty} \int_0^\infty P_{pos}(y) \int_{|t_{A2} - t_{A1} - y|}^\infty G(x|n_m, \lambda) dx dy = 0. \quad (4)$$

Let $(\alpha_n)_n$ be a sequence of real numbers, such that $\alpha_n \rightarrow \infty$ as $n \rightarrow \infty$. Let $(f_n)_n$ be the sequence of functions, such that for all $n \in \mathbb{N}$ and $y \in \mathbb{R}^+$,

$$f_n(y) = P_{pos}(y) \int_{|t_{A2} - \alpha_n - y|}^\infty G(x|n_m, \lambda) dx.$$

As $n \rightarrow \infty$, f_n converges pointwise towards 0. In addition, for all $n \in \mathbb{N}$ and $y \in \mathbb{R}^+$, $|f_n(y)| \leq P_{pos}(y)$, where P_{pos} is integrable on \mathbb{R}^+ . A standard application of the dominated convergence theorem yields

$$\lim_{n \rightarrow \infty} \int_0^\infty f_n(y) dy = 0.$$

As the latter is true for any sequence (α_n) , (4) is proved.

The reasoning is identical for the second part of the expression.

$$\lim_{t_{A1} \rightarrow \infty} \int_{-\infty}^0 P_{neg}(y') \int_{|t_{A2}-t_{A1}-y'|}^{\infty} G(x'|n_m, \lambda) dx' dy' = 0 \quad (5)$$

Therefore, from (4) and (5), we obtain that for a node, $f(t_{A1}) \rightarrow 0$ as $t_{A1} \rightarrow \infty$.

Edge constraints For an edge, let us also define $(\alpha_n)_n$ a sequence of real numbers such that $\alpha_n \rightarrow \infty$ as $n \rightarrow \infty$. Let $(g_n)_n$ be the sequence of functions such that $\forall n \in \mathbb{N}, \forall e_2 \in \mathbb{R}^+$:

$$g_n(e_2) = G(e_2|n_1, \lambda) \int_{(h_n(e_2)-t_e)^+}^{(h_n(e_2)+t_e)^+} G(x|n_2, \lambda) dx$$

with

$$h_n(e_2) = e_2 + t_{A2} - \alpha_n$$

$(g_n)_n$ converges pointwise towards f_0 . Let us define g_1 such that $\forall e_2 \in \mathbb{R}^+$, $g_1(e_2) = G(e_2|n_1, \lambda)$. Then g_1 is integrable on \mathbb{R}^+ and $\forall e_2 \in \mathbb{R}^+$, $|g_n(e_2)| \leq g_1(e_2)$. Thus the theorem of dominated convergence also applies and we obtain $f(t_{A1}) \rightarrow 0$ as $t_{A1} \rightarrow \infty$.

Finally, as we take steps of size Δt until the probability becomes smaller than ϵ , then for any $\delta \in \mathbb{R}^{+*}$, we are able to find $\Delta t \in \mathbb{R}^{+*}$ and $k \in \mathbb{N}$ such that $P_{ce}(t_1 + k\Delta t, n_1, t_2, n_2) \in [\epsilon - \delta, \epsilon]$. Therefore, we have proved Lemma 1. \square

Lemma 2 *Let N be a node with a non-empty set of constraints, an optimal solution $s \in CV(N)$ returned by A^* , and children N_1 and N_2 . Let p be a valid solution. Then if $p \in CV(N)$, then at least one of the following is true: $p \in CV(N_1)$ or $p \in CV(N_2)$*

Proof. Let t_{A1} and t_{A2} be the planned times of conflicting agents R1 and R2 at the element of interest. Since $p \in CV(N)$, we know that none of N .constraints are violated. We know that R1 cannot arrive at the element before t_{A1} , and R2 cannot arrive before t_{A2} . Let t_{D1} be the delay for agent R1 that brings the conflict probability to ϵ while agent R2 remains on its shortest path, and t_{D2} the delay for agent R2 that brings the conflict probability to ϵ while agent R1 remains on its shortest path.

We know that we are able to find such times by using Lemma 1. More precisely, for a node, with $\delta = t_{A1} - t_{A2}$, we know that $P_{cm}(\delta, n_1, n_2, n_m, \lambda) \rightarrow 0$ as $\delta \rightarrow \infty$, and $P_{cm}(\delta, n_1, n_2, n_m, \lambda) \rightarrow 0$ as $\delta \rightarrow -\infty$. The same applies for an edge.

Then, we can show that there is no valid solution for which planned times for R1 and R2 will each belong to $[t_{A1}, t_{D1}[$ and $[t_{A2}, t_{D2}[$, respectively. In other words, a solution with such planned arrival and departure times has a conflict probability greater than ϵ . We can easily state this with the methodology we

used in order to find t_{D1} and t_{D2} : we advance of steps size Δt until we find a conflict probability smaller than ϵ . Thus, we know that when $\Delta t \rightarrow 0$, if $t_{D2} - (t_{A1} - t_{A2}) < \delta < t_{D1} - (t_{A1} - t_{A2})$, the corresponding conflict probability is strictly greater than ϵ . Finally, because we cannot choose planned arrival times that are inferior to t_{A1} and t_{A2} for both agents, we can conclude that one of the new arrival times planned for agents R1 and R2 needs to be larger than t_{D1} or t_{D2} , respectively. Therefore, for a valid solution, at least one of the additional constraints for planned arrival time is verified.

If we are to search for t_{D1} and t_{D2} using a more efficient method such as binary search, the Lemma still holds and the proof includes demonstrating the unimodality of $\delta \mapsto P_{cm}(\delta, n_1, n_2, n_m, \lambda)$. \square

Lemma 3 *The path returned by A^* for a given node N is a lower bound on $\min(\text{Cost}(CV(N)))$*

Proof. A^* returns the solution S verifying all constraints of N , and minimizing the sum of expected travel times, which is the same as the expected sum of travel times. Therefore, the cost of S is a lower bound on the cost of solutions that do not violate constraints of N . However, we know that $CV(N)$ is a subset of this set. Therefore, the cost of S is a lower bound on the minimum cost of an element in $CV(N)$. \square

Lemma 4 *Let p be a valid solution. At all time steps there exists a node N in the priority queue that permits p .*

Proof. We reason by induction on the expansion cycle [1].

Base case: At first, the priority queue (called *OPEN* in [1]) only contains the root node, which has no constraints. Consequently, the root node permits all valid solutions and also p .

Heredity: Let us assume this is true for the first i expansion cycles, and call N the concerned node in the priority queue that permits p . In cycle $i + 1$, if node N is not expanded, it remains in the priority queue, in which case the priority queue still permits p . On the other hand, let us assume that node N is expanded and its children N_1 and N_2 are generated. Then, using Lemma 2, we can state that any valid solution for N must be solution for N_1 or N_2 . In both cases, there exists a node in the priority queue at the next expansion cycle that permits p .

Conclusion: For any valid solution p , at least one constraint tree node in the priority queue permits p .

By extension, there is always a node in the Priority Queue that contains the optimal solution. \square

Theorem 1 *As $\Delta t \rightarrow 0$, STT-CBS returns the optimal solution with respect to the expected cost that ensures each pairwise conflict probability is smaller or equal to ϵ .*

Proof. Let us consider the algorithm returns a valid solution g from a goal node G . We know that at all times, all valid solutions are permitted by at least one

node from the priority queue (Lemma 4). Let p be a valid solution (with cost $c(p)$) and let $N(p)$ be the node that permits p in the priority queue. Let $c(N)$ be the cost of node N . We have $c(N(p)) \leq c(p)$ (Lemma 3). We know that, since g is valid, $c(G)$ is a cost of a valid solution. Finally, as in [1], the search algorithm explores solution costs in a best-first manner. Due to this, we get that $c(g) \leq c(N(p)) \leq c(p)$, which proves Theorem 1. \square

5 Simulations and Experiments

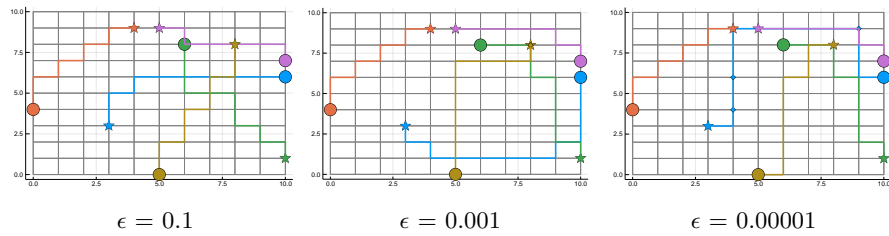


Fig. 3: Solutions for STT-CBS on a 10×10 grid for 5 agents, with different values of ϵ . Paths start at the stars, end at the circles, and are paused at the diamonds. With no uncertainty, each edge takes 1 time step to traverse.

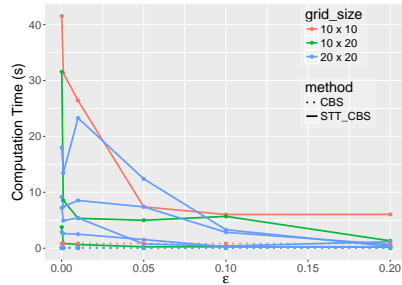


Fig. 4: Computation time on a set of examples for different values of ϵ on problems with 10 agents and three different grid sizes. The dotted lines represent computation times for CBS applied to the same problems.

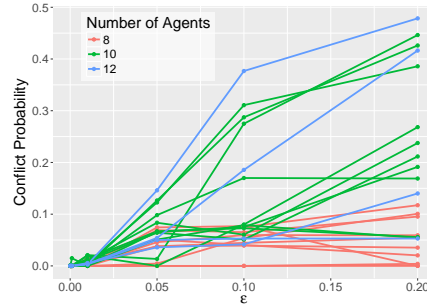


Fig. 5: Global conflict probability evaluated for a number of agents varying between 8 and 12. We choose $\lambda = 5$ and $n_m = 1$ at all nodes.

Figure 3 shows the effect of ϵ on the returned solution, for an experiment on a 10×10 grid containing 5 agents.

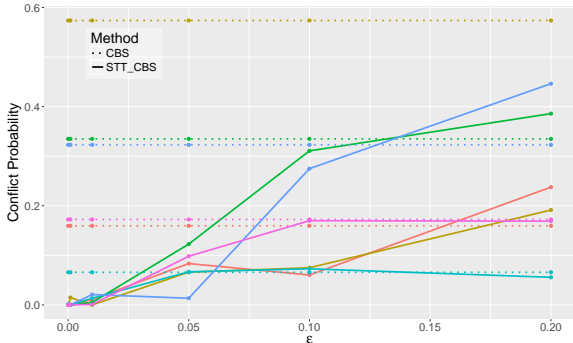


Fig. 6: Conflict probability comparison for 10 agents. Each color represents a specific trial.

Computation time Figure 4 shows computation time results for CBS and STT-CBS with different values of ϵ . These experiments were performed on 10×10 , 10×20 , and 20×20 grids. We note that with large values of ϵ , both problems are almost equivalent.

Conflict Probability We have evaluated the global conflict probability on the full considered time horizon on a set of experiments, as a function of ϵ . Figure 5 show that in general, decreasing ϵ decreases global conflict probability. Figure 6 compares the results with CBS directly. The conflict probabilities found with CBS are significantly larger than those found with STT-CBS and reasonable values of ϵ .

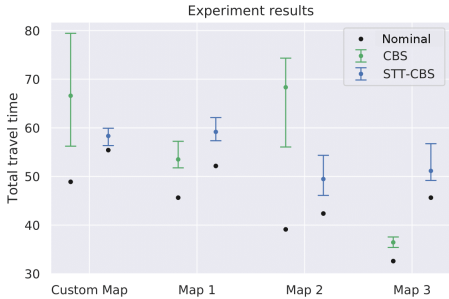


Fig. 7: For each map and algorithm, 4 trials were conducted. The colored dots represent the mean. The error bars represent the minimum and maximum sampled values. Travel times are in seconds.

Hardware experiments In order to test our algorithm, we use the OuijaBot [26]—a custom-designed omnidirectional platform—to execute solutions. To avoid col-



a) STT-CBS



b) CBS

Fig. 8: We compare two different solutions computed by STT-CBS and CBS for the same problem in a 5×5 custom environment. At each time step, we compare agents' actual (upper) and simulated (lower) positions. We notice that the solution returned by CBS requires the agents to navigate close to one another as they follow each other. During the execution, agents are not able to perform this maneuver without risking collision and compute alternate routes to avoid each other. In contrast, STT-CBS returns a slightly more expensive solution that the agents are able to execute safely.

lisions, we plan trajectories using Reciprocal Collision Avoidance for Real-Time Multi-Agent Simulation [27]. In the experiments, three robots are instructed to follow way-points. Travel time is uncertain as their dynamics vary with time, battery level, and floor condition, and they need to avoid each other. Consequently, the distribution for agent delay is unknown and realistic.

We compare the performance of CBS and STT-CBS in one custom environment, and three chosen among 10 randomly generated environments where CBS and STT-CBS yield significantly different solutions. We chose $n = 1$ and $\lambda = 5$ to model delay, and $\epsilon = 0.1$ as conflict probability threshold. The results are summarized in Figure 7, where the nominal cost was computed using the nominal robot velocity with no delay. We find that the additional safety provided by STT-CBS helps the observed costs to vary significantly less, and consistently approach the nominal cost (i.e. the cost with no stochastic delay in travel times). Figure 8 illustrates a difficulty that becomes apparent when the computed path is not sufficiently robust to travel time uncertainty.

6 Conclusion

STT-CBS offers quantifiable robustness to stochastic travel time delays in realistic multi-agent path finding scenarios compared with the standard CBS method, while minimizing the expected solution cost. In future work, we plan to combine STT-CBS with task assignment to obtain a simultaneous assignment and path finding algorithm (see, e.g., CBS-TA [2] and CBM [12]) with robustness to stochastic travel times and other realistic disturbances.

References

1. Sharon, G., Stern, R., Felner, A., Sturtevant, N.R.: Conflict-based search for optimal multi-agent pathfinding. *Artificial Intelligence*, Volume 219, Pages 40-66 (2015)
2. Hnig, W., Kiesel, S., Tinka, A., Durham, J.W., Ayanian, N.: Conflict-Based Search with Optimal Task Assignment. In *Proceedings of the 17th International Conference on Autonomous Agents and Multi-Agent Systems (AAMAS)*. International Foundation for Autonomous Agents and Multiagent Systems, 757765 (2018)
3. Felner, A., Li, J., Boyarski, E., Ma, H., Cohen, L., Kumar, T. S., Koenig, S.: Adding heuristics to conflict-based search for multi-agent path finding. *International Conference on Automated Planning and Scheduling* (2018)
4. Li, J., Harabor, D., Stuckey, P. J., Ma, H., Koenig, S.: Disjoint splitting for multi-agent path finding with conflict-based search. *International Conference on Automated Planning and Scheduling*, Vol. 29, No. 1, pp. 279-283 (2019)
5. Surynek, P.: Unifying search-based and compilation-based approaches to multi-agent path finding through satisfiability modulo theories. In *Twelfth Annual Symposium on Combinatorial Search* (2019)
6. Kornhauser, D., Miller, G., Spirakis, P.: Coordinating pebble motion on graphs, the diameter of permutation groups, and applications. Cambridge, MA, USA, Technical Report (1984)
7. Čáp, M.: Centralized and Decentralized Algorithms for Multi-Robot Trajectory Coordination (2017)

8. Yu, J., LaValle, S. M.: Optimal multirobot path planning on graphs: Complete algorithms and effective heuristics. *IEEE Transactions on Robotics*, 32(5), 1163-1177 (2016)
9. Krichene, W., Reilly, J., Amin, S., Bayen, A.: On the characterization and computation of Nash equilibria on parallel networks with horizontal queues. *IEEE Conference on Decision and Control (CDC)* (pp. 7119-7125) (2012)
10. Atzmon, D., Stern, R., Felner, A., Wagner, G., Bartk, R., Zhou, N. F.: Robust multi-agent path finding. In *Eleventh Annual Symposium on Combinatorial Search* (2018)
11. Yu, J.: Intractability of optimal multirobot path planning on planar graphs. *IEEE Robotics and Automation Letters*, 1(1), 33-40 (2015)
12. Ma, H., Koenig, S.: Optimal target assignment and path finding for teams of agents. *arXiv preprint:1612.05693*. (2016)
13. De Wilde, B., Ter Mors, A.W., Witteveen, C.: Push and rotate: a complete multi-agent pathfinding algorithm. *Journal of Artificial Intelligence Research*, 51, pp.443-492 (2014)
14. Standley, T.S., Korf, R.: Complete Algorithms for Cooperative Pathnding Problems. *International Joint Conference on Artificial Intelligence* (2011)
15. Yu, J.: Intractability of optimal multirobot path planning on planar graphs. *IEEE Robotics and Automation Letters*, 1(1), 33-40 (2015)
16. Wurman, P. R., D'Andrea, R., Mountz, M.: Coordinating hundreds of cooperative, autonomous vehicles in warehouses. *AI magazine*, 29(1), 9-9 (2008)
17. Ashayeri, J., Gelders, L. F.: Warehouse design optimization. *European Journal of Operational Research*, 21(3), 285-294 (1985)
18. Ho, F., Geraldes, R., Goncalves, A., Cavazza, M., Prendinger, H.: Simulating shared airspace for service UAVs with conflict resolution. *International Conference on Autonomous Agents and MultiAgent Systems* (pp. 2192-2194) (2018)
19. Samaranyake, S., Blandin, S., Bayen, A.: A tractable class of algorithms for reliable routing in stochastic networks. *Transportation Research Part C: Emerging Technologies*, 20(1), 199-217 (2012)
20. Lumelsky, V. J., Harinarayan, K. R.: Decentralized motion planning for multiple mobile robots: The cocktail party model. *Autonomous Robots*, 4(1), 121-135. (1997)
21. Hart, P. E., Nilsson, N. J., Raphael, B.: A formal basis for the heuristic determination of minimum cost paths. *IEEE transactions on Systems Science and Cybernetics*, 4(2), 100-107 (1968)
22. Yu, J., LaValle, S. M.: Structure and intractability of optimal multi-robot path planning on graphs. *AAAI Conference on Artificial Intelligence* (2013)
23. Li, J., Surynek, P., Felner, A., Ma, H., Kumar, T. S., Koenig, S.: Multi-agent path finding for large agents. In *Proceedings of the AAAI Conference on Artificial Intelligence* (Vol. 33, pp. 7627-7634) (2019)
24. Wagner, G., Choset, H.: Path planning for multiple agents under uncertainty. *International Conference on Automated Planning and Scheduling* (2017)
25. Wagner, G., Choset, H.: M*: A complete multirobot path planning algorithm with performance bounds. In *2011 IEEE/RSJ international conference on intelligent robots and systems* (pp. 3260-3267) (2011)
26. Wang, Z., Yang, G., Su, X., Schwager, M.: Oujabots: Omnidirectional robots for cooperative object transport with rotation control using no communication. In *Distributed Autonomous Robotic Systems* (pp. 117-131). Springer, Cham. (2018)
27. Van Den Berg, J., Guy, S. J., Lin, M., Manocha, D.: Reciprocal n-body collision avoidance. In *Robotics research* (pp. 3-19). Springer, Berlin, Heidelberg (2011)